

A 400 N Bipropellant Thruster with Swirl Injectors

J N Hinckel and C F Wehmann†*

**Senior Researcher † Visiting Researcher*

INPE - SJC SP BR

Abstract

This paper describes the development status of a 400 N thrust bipropellant engine. The thruster uses the storable propellants NTO/MMH (Nitrogen Tetroxide/Mono methyl Hydrazine). The injector head uses a combination of monopropellant and bipropellant swirl injector elements. Seven (1+6) counter swirling bipropellant injector elements are located in the center region. 12 fuel swirl injectors are placed in a peripheral ring. The thrust chamber material is niobium and is coated on the internal and external surfaces with a thin layer of niobium aluminide. The main application for the thruster is in apogee acceleration block for geostationary satellites.

1. Introduction

The main challenge presented to the designer of small thrust bipropellant thruster engines is the balance between the energetic efficiency of the thruster and the thermal protection of the chamber wall. Due to operational constraints and a deficit of cooling capacity, active cooling of the chamber wall is not a viable option for thermal protection. The radial stratification of the propellant mixture ratio is the technique most widely used to satisfy the competing requirements. A fuel (or oxidizer) rich mixture near the chamber wall reduces the heat load on the chamber wall. A near stoichiometric mixture ratio in the core improves the energetic efficiency of the thruster. The design of the injector head is the single most important means of achieving this delicate balance. The use of materials with high strength at high temperature is also required for high energetic efficiency.

2. Design and Construction

2.1 The geometry of the thrust chamber

The operating input parameters for the design of the thrust chamber are the nominal thrust, 400 N, the nominal chamber pressure, 1 MPa, the oxidizer to fuel mass flow ratio, 1.25, and the nozzle pressure expansion ratio, 1000:1.

The characteristic length is assigned a value of $L^* = 0.9$ m. The combustion and expansion efficiency are assigned values of $\varphi_{ch} = 0.97$ and $\varphi_n = 0.98$, respectively. The combined efficiency is $\varphi = 0.95$.

The diameter of the throat and the combustion chamber volume are then calculated from these parameters using standard formulas.

An empirical formula relating the chamber pressure, thrust level and throat diameter is used to calculate the diameter of the combustion chamber. The resulting meridional cross section of the chamber is approximately square. To increase the traveling distance of the injector spray and prevent the high heat release near the chamber wall a slightly spherical chamber is used instead of a straight cylinder.

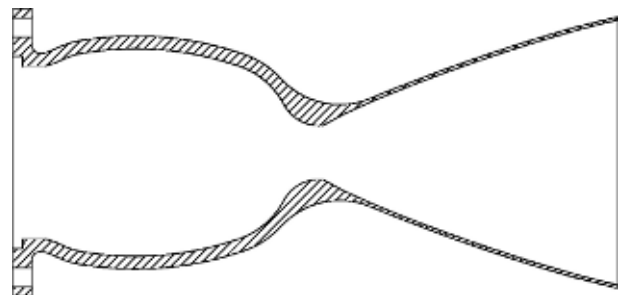


Figure 1: Geometry of the thrust chamber

The throat section has a short cylindrical section and a sharp opening to the starting nozzle. The expansion nozzle has a parabolic shape. The geometry of the parabola is defined by a starting exit angle, throat and exit diameter and nozzle length. The starting angle is the maximum turning angle for nominal nozzle area ratio. The exit angle is an arbitrary choice. For a given nozzle area ratio a larger exit angle results in a shorter nozzle, although with increased losses of expansion efficiency. Tabulated values from [4] are used to define the parabolic arc. A 10° exit angle was used.

The thrust chamber was machined from a solid niobium cylinder. To reduce the amount of machining a nozzle with expansion area ratio of 24:1 instead of the nominal 62:1 was used. To produce the high area ratio nozzle the exit part of the nozzle must be produced by a sheet forming method. The geometry of nozzle is shown in figure 1.

To protect the chamber wall from possible oxidizer rich propellant mixture reaching the wall or from ambient oxygen, the thrust chamber is covered on the inside and outside surface with a protective layer of niobium aluminide. The thickness of the protective layer depends on the deposition process. An initial aluminum layer is deposited on the surface of the chamber. The chamber is then heated in a high temperature furnace and the aluminum film reacts with the niobium wall forming a layer of niobium aluminide.

2.2 The injection head

The layout of the injector elements on the injector head has a single bipropellant element in the center of the head and six additional bipropellant elements are placed in an intermediate ring. Twelve fuel monopropellant elements are placed in a outer ring.

The total mass flow is calculated from the overall mass ratio and estimated losses of the characteristic velocity and the thrust coefficient.

The starting point for the design is the target overall mass ratio of the thruster. The injector elements of the outer ring are assigned a mass flow of 2 g/s. The balance of the fuel and all of the oxidizer are equally divided in 7 central bipropellant injectors. The desired mass flow ratio of the bipropellant elements is the stoichiometric ratio. If the resulting value for the overall mass ratio is very far from the desired value a new target overall mass flow ratio is chosen and the calculation is repeated.

The injector head is composed of three plates; a distribution plate, a fuel plate and an oxidizer plate. The distribution plate contains the entrance ports for the fuel and oxidizer. The swirl chambers for the injector elements are machined on the face of the fuel plate and oxidizer plate. The three plates are joined by vacuum diffusion welding. The oxidizer plate is sandwiched between the distribution plate and the fuel plate.

The layout of the injector elements on face of the injector plates is constrained by considerations related to the load distribution during the diffusion welding process and the sealing between the fuel and oxidizer feed labyrinths.

A protruding tube is attached to the exit nozzle of each oxidizer element. By changing the length of the tube, the impinging distance of the oxidizer and fuel spray sheets can be controlled. The exit face of the oxidizer nozzle is recessed with respect to the fuel nozzle exit face. Depending on the recess distance the impinging point may be located inside the fuel nozzle or outside the nozzle.

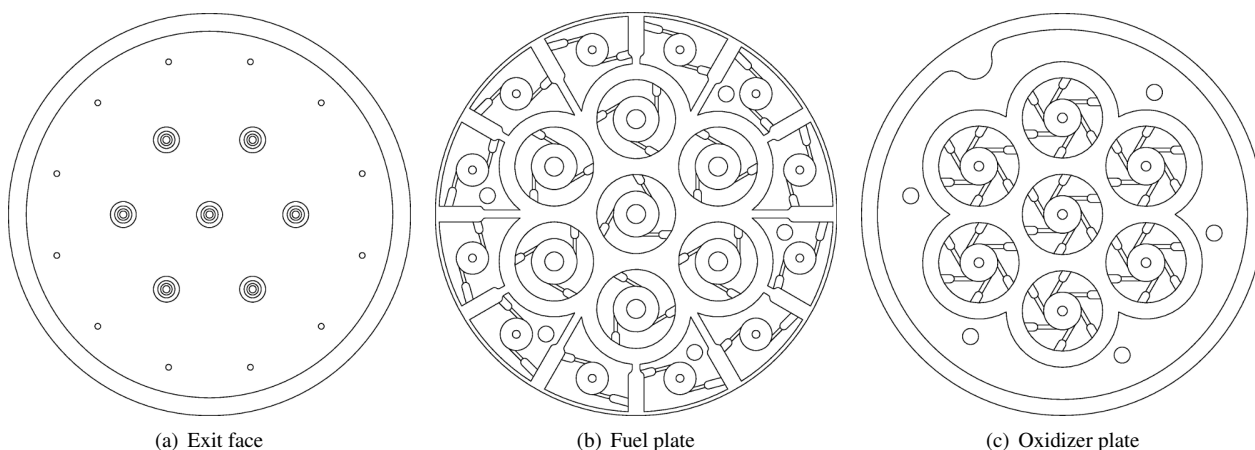


Figure 2: Head

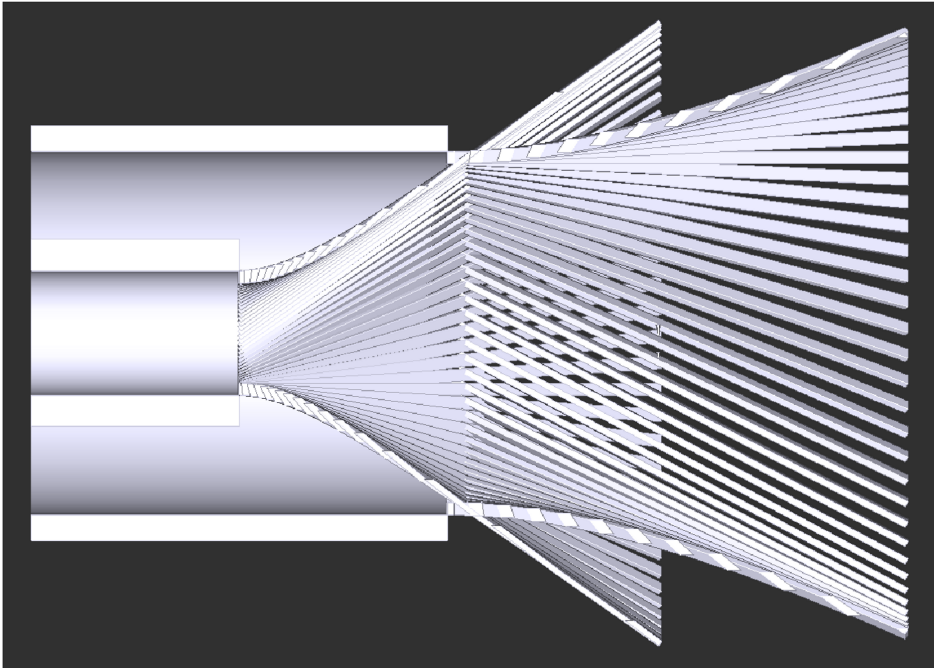


Figure 3: Artistic representation of the duplex injector spray sheets

The inside angle of the “conical” spray sheet increases monotonically with the geometric parameter A of the injector in the original calculation procedure derived by Abramovitch [4]. From considerations related to the dimensional and construction constraints it results that the value of the geometric parameter of the outside injector element is greater than the value of the geometric parameter of the inside injector element (in the duplex configuration).

Several techniques are used to decrease the angle of the “conical” spray sheet for a fixed value of the geometric parameter A . By contouring the exit section of the nozzle of the outside injector element it is possible to reduce the angle of the outside sheet to a value smaller than the angle of the inside sheet.

An artistic representation of the spray sheet is depicted in Figure 3.

The fuel and oxidizer chambers swirl in opposite directions to increase the relative velocity of the fuel and oxidizer spray sheets and to minimize the overall angular momentum injected into the thrust chamber.

Figure 2 shows the view of the injector head and the layout of the swirl chambers in the fuel and oxidizer plates.

3. Testing and Results

3.1 Cold Flow Test

A number of test procedures was used to characterize and evaluate the behavior of the thruster. Besides a full inspection of the machined parts, an extensive set of tests was used to evaluate the quality of the propellant spray.

A series of cold tests was carried out to ensure that the propellant spray characteristics were favorable to the uniform mixing of the propellant and to prevent the appearance of hot spots in the chamber.

The mass flow rate of each individual injector element is measured before and after the diffusion welding process. The main purpose of this test is to assert that the design mass flow of each injector element and overall mass flow are attained. The mass flow ratio of each bipropellant element and the overall mass flow ratio are also verified in this test.

Table 1 shows the measured mass flow rate for each injector element at the nominal pressure drop of 0.5 MPa, after the welding process. For the 7 inner bipropellant elements, the mass ratio is also shown. Element 1 is in the center, elements 2 to 7 are in the intermediate ring and elements 8 to 19 form the outer ring.

The nominal inviscid, Nom_{inv} , and nominal viscous, Nom_{visc} , calculated values of injector elements mass flow rate are shown. Nom_{inv} are the calculated values for the inner bipropellant injector elements using the calculation procedure described in [2] for “simplex swirl atomizers”. Nom_{visc} are the corresponding values corrected for viscous effects according to calculation procedures from the same reference.

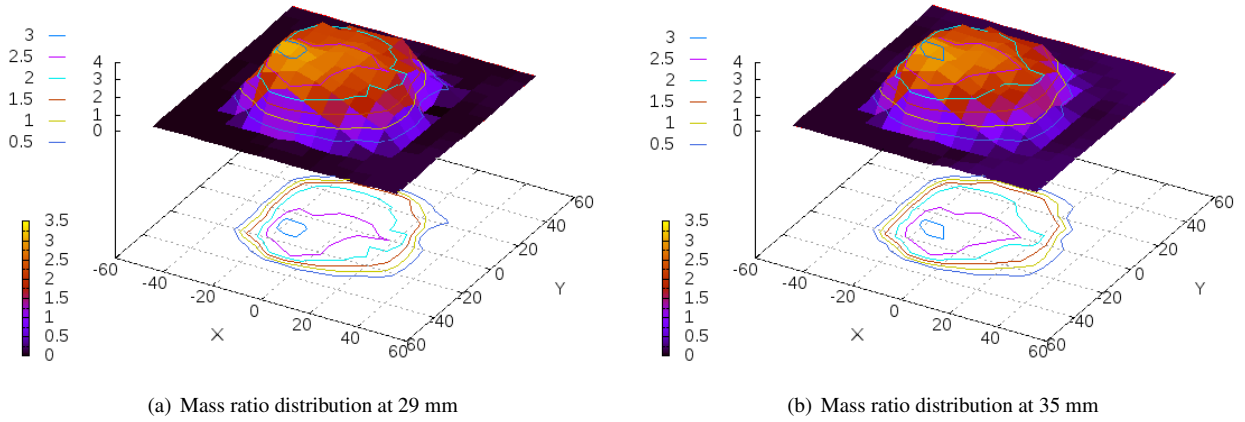


Figure 4: Radial distribution of mixture ratio

The viscosity correction brought the calculated values closer to the measured values in the case of the periphery injector elements and the inner oxidizer elements. For the inner fuel injector elements the measured value of the mass flow rate was closer to the results obtained from the standard calculation procedure than to the results of calculation with viscosity effects correction.

The accuracy of analytical and numerical calculation methods of swirl injectors and experimental verification is reported in [3].

The measured overall mass ratio for the nominal injector pressure drop was 1.1.

The radial and azimuthal mixture ratio distribution is also measured. The cold spray of an ethanol/water mixture is collected in a cylindrically arranged matrix. A high accuracy densimeter is used to determine the distribution of the mixture ratio from the local density measurement.

All the collecting elements have the same cross sectional area. There is one central element and 5 concentric rings of collection elements. The first ring contains 6 elements. Each successive ring has 6 additional collecting elements.

Figure 4 illustrates the measured mixture ratio for one of injector heads at different distances from the injector face. The data depicted in the figures are not corrected for density of the actual propellants. Therefore, the qualitative shape of the level curves should not change but the quantitative values will be changed for the actual propellants.

3.2 Hot Fire Tests

Hot firing tests were carried out in a test stand with altitude simulation capability. The vacuum system includes mechanical pumps for initial pump down, two parallel lines with series mounted vapor ejectors, one condenser, liquid ring pumps and residual exhaust gas treatment. The vacuum system operates in continuous mode during a test sequence.

The vacuum system pump down, propellant pressurization and engine start are commanded by a dedicated computer. The display of the thruster instrumentation data and the acquisition of the test data are handled by a separate computer.

The following data are acquired during the test at fast rate: fuel and oxidizer lines feed pressure and flow rate, valve current and voltage, thrust chamber pressure, environment chamber back pressure. The temperature of the

Duplex injector elements			
N_e	\dot{m}_f [g/s]	\dot{m}_o [g/s]	φ
1	5.96	11.44	1.92
2	5.68	11.74	2.07
3	5.54	11.20	2.02
4	5.45	11.09	2.04
5	5.35	11.15	2.08
6	5.67	11.43	2.02
7	5.19	11.88	2.25
Nom_{inv}	5.25	10.51	2.0
Nom_{visc}	7.12	10.74	1.7
Single injector elements			
N_e	\dot{m} [g/s]	N_e	\dot{m} [g/s]
8	2.70	14	2.61
9	2.56	15	2.65
10	2.46	16	2.73
11	2.47	17	2.74
12	2.43	18	2.71
13	2.57	19	2.71
Nom_{inv}	2	Nom_{visc}	2.44

Table 1: Nominal and measured injector elements mass flow rate

propellant feed and the temperature of the outside surface of the thrust chamber (if instrumented with thermocouples) are acquired at slow rate.

The propellant valves are mounted with threaded fittings to connectors welded to the distribution plate of the injector head. The valves are normally closed with spring load closing and an electrical coil actuated poppet.

The opening and closing commands for the propellant valves are independent. A 10 ms lead time is applied to the fuel valve during opening command to ensure a fuel lead feed in the injector head and combustion chamber. Closing commands are simultaneous.

The thruster is mounted to the thrust balance in the vertical position with the exhaust nozzle pointed downward. A water cooled plate deflects the exhaust stream to the vacuum system entrance port. Figure 5 shows the thruster mounted on the test stand.

After the firing a nitrogen gas jet is directed against the back face of the injector plate and valves to avoid overheating from thrust chamber heat soak back.

The feed pressure of both propellants is changed independently to obtain different values of the mixture ratio.

Figure 6 shows the chamber pressure and thrust trace during one 15 s shot.



Figure 5: 400 N engine mounted on test stand

4. Test results and analysis

Table 2 shows the results for one sequence of firing tests with different feed pressures. P_f is the fuel feed pressure, P_o , the oxidizer feed pressure, P_c , the combustion chamber pressure, k_m , the oxidizer to fuel mass ratio, I_{sp} , the specific impulse, I_{sp}^{id} , the ideal specific impulse, c^* , the characteristic velocity and C_f the thrust coefficient, $I_{sp}(200 : 1)$, the specific impulse projected to a nozzle expansion area ratio of 200:1.

The initial series of tests had a duration of 5 s. The purpose of these tests was to map the performance of the thruster over an envelope of the mixture ratio and chamber pressure by using different combinations of values of the feed pressure for oxidizer and fuel lines.

The longest test for this engine was 15 s. The test duration was limited by the altitude simulation system which was operating with only one of the two parallel vapor ejector lines. The expected operating life of the thruster is 2000 s accumulated operating time, at least 20 engine starts and longest firing time of at least 200 s.

The maximum chamber temperature measured during the test was approximately 1000°C. Extrapolation of external surface temperature to steady state Conditions projected a maximum value of 1200°C. The analysis of the

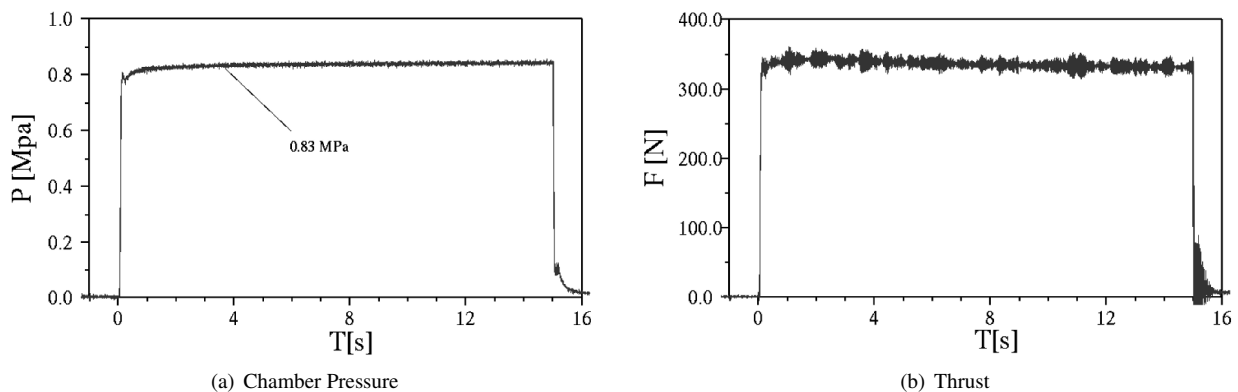


Figure 6: Chamber Pressure and Thrust for a 15 second test

Test №	Thrust	P_f	P_o	P_c	\dot{m}	k_m	I_{sp}	I_{sp}^{id}	c^*	C_f	$I_{sp}(200 : 1)$
	N	Bar	Bar	Bar	g/s		m/s	m/s	m/s	m/s	m/s
01	294.1	17.92	15.04	7.42	114.8	1.205	2561	2893	1428	1.79	2866
02	304.1	19.97	15.02	7.65	117.2	1.065	2595	2819	1442	1.80	2919
03	310.3	22.03	15.02	7.76	122.3	1.004	2538	27812	1403	1.81	2865
04	307.7	18.16	16.09	7.60	115.0	1.326	2675	2944	1461	1.83	2992
05	320.7	19.09	17.15	7.89	122.7	1.286	2614	2929	1421	1.84	2923
06	327.4	20.03	17.16	8.02	123.0	1.203	2662	2893	1441	1.85	2979
07	330.5	20.94	17.16	8.10	124.7	1.149	2664	2869	1443	1.85	2985
08	333.7	21.97	17.15	8.20	126.3	1.106	2641	2846	1434	1.84	2965
09	331.0	18.70	17.13	8.22	127.9	1.281	2588	2929	1429	1.82	2905
10	323.8	18.70	16.90	8.14	125.1	1.249	2588	2929	1438	1.80	2905
11	317.8	18.80	16.90	8.12	124.1	1.236	2561	2929	1446	1.77	2875
12	317.5	18.40	16.90	8.15	126.2	1.271	2515	2929	1427	1.76	2823
13	300.0	18.50	18.70	8.30	127.6	1.458	2586	2985	1437	1.80	2897

Table 2: Hot firing test results for different propellant feed pressure

thermal load on the thrust chamber wall is presented in [1]. The analysis uses an inverse method solution to obtain the thermal load on the inner surface of the thrust chamber. The outer surface temperature of the chamber is mapped during the transient heating with an infrared camera. An inverse method algorithm is used in conjunction with the solution of the heat diffusion in the chamber to obtain the axial distribution of the heat transfer coefficient and the near wall film temperature. The heat load implied by these profiles is used to extrapolate the steady state condition. The steady state temperature on the chamber wall is attained in approximately 20 s.

The niobium aluminide layer did not show any sign of degradation or loss of adhesion after the series of 30 firing shots.

The thrust level was noticeably lower than the nominal 400 N value. The main reasons for this are that the expansion nozzle area ratio used was 24:1 instead of the 62:1 design value and, the lower than nominal chamber pressure of 10 bar. The main reason for the reduced chamber pressure was the high pressure drop of the propellant valves used in this test and hence lower propellant mass flow rate.

The last column of Table 2 contains the expected specific impulse data extrapolated to operating conditions in vacuum for a nozzle expansion ratio of 200:1. The extrapolation condition was that with the higher area ratio nozzle the losses of characteristic velocity and nozzle expansion would not be affected.

5. Conclusions

A nominal 400 N bipropellant thruster engine with swirl injector elements head was produced and tested. The engine was tested with the storable propellant pair NTO/MMH (Nitrogen Tetroxide / Mono-methyl Hydrazine). 7 bipropellant injector elements are placed in the center region of plate. A ring of 12 monopropellant injector elements is placed in the periphery of the injector plate. This injector elements layout creates a radially stratified mixture ratio spray of propellants.

The swirl injector elements and the feed manifold are machined on the face of the fuel plate and oxidizer plates. A distribution plate directs the propellants to plates. A central injector dome in the distribution plate feeds the oxidizer to the manifold in the oxidizer plate. The fuel is directed to a fuel ring on the periphery of the injector head.

The injector plates; distribution, oxidizer and fuel, are stacked and welded together by a vacuum diffusion bonding process. The layout of the injector elements and manifolds on the surface to plates must distribute the load applied to the plates during the diffusion bonding process.

The thrust chamber was machined in niobium and had a protective layer of niobium aluminide on the inside and outside. No damage to the protective layer was observed after a series of test with 30 engine starts and accumulated test time of 200 seconds.

The thruster was fired in a test facility with altitude simulation capability. By changing the feed pressure of the oxidizer and fuel independently the overall oxidizer to fuel mass flow ratio was changed in the range of 1.0 to 1.4. The

chamber pressure for all tests was in the range of 7.4 to 8.3 bar. The decision on the operational value of the mixture ratio will depend on the maximum temperature of the thrust chamber wall. Small changes to the injector layout and feed manifold are being pursued in order to improve the thermal protection of the wall with minimal losses of energetic performance.

The chamber pressure roughness was small for the range of mixture ratio and thrust levels tested. The pressure buildup during the engine start and the pressure decay during engine shut down was smooth, without overshooting or spikes.

The main application for this engine is in apogee acceleration blocks for geostationary bound satellites. For this application the thrust chamber material will be niobium with a protective layer of niobium aluminide; the expansion area ratio will be 200:1.

Acknowledgment. This work was supported by FAPESP PN 2003/06878-6 and CNPq PN 303359/2006-4.

References

- [1] 4th European Conference for Aerospace Sciences. *Determination of Thermal Load in Film Cooled Bipropellant Thrust Chambers by an Inverse Method*, number Eucass 2011-421, Saint Petersburg, July, 4-8 2011.
- [2] L. Bayvel and Z. Orzechowski. *Liquid Atomization*. Taylor & Francis, 1993.
- [3] J. N. Hinckel, V. G. Bazarov, and H. F. Villa Nova. Cfd analysis of swirl atomizers. Number AIAA 2008-5229, Hartford, CT, July, 21-23 2008. 44th AIAA/ASME/SAE/ASEE Joint Propulsion Conference & Exhibit.
- [4] A. P. Vasiliev, V. M. Kudriavtzev, V. A. Kuznetsov, V. D. Kurpatenkov, A. M. Obelnitsky, V. M. Poliaev, and B. I. Poliaev. *Osnoviy Teorii y Rascheta GRD (in Russian)*. Moskwa Visshaia Shkola, 1993.